



Numerical Analysis of Single Edge Notched Tension Specimen with Fatigue Crack Parameter of Conventional Specimen Using Linear Elastic Fracture Mechanics

Yusuf Olanrewaju Busari^{1,2*}, Shahrum Abdullah³, Yupiter H.P. Manurung¹,
Yusuf Lanre Shuaib-Babata²

¹Smart manufacturing Research Institute, Faculty of Mechanical Engineering,
Universiti Teknologi MARA, (UiTM), Shah Alam, Selangor, 40450, MALAYSIA

²Department of Materials and Metallurgical Engineering,
University of Ilorin, P.M.B. 1515, NIGERIA

³Faculty of Engineering and Built Environment,
Universiti Kebangsaan Malaysia, Bangi, Selangor, 43600, MALAYSIA

*Corresponding Author

DOI: <https://doi.org/10.30880/ijie.2021.13.07.018>

Received 16 August 2021; Accepted 2 September 2021; Available online 30 September 2021

Abstract: This paper describes the numerical analysis of planar crack growth in high strength steel API 5L X70 whose crack growth parameter is adopted from experimental compact tension (CT) specimen in previous literature. Apart from the fact that conventional fatigue crack growth specimen has bogus geometry constraints, the Single Edge Notched Tension (SENT) better replicate the crack-tip constraint conditions experienced in structures. Linear elastic fracture mechanics (LEFM) crack orientation is modelled with the finite element method in SENT model considering its geometry functions a/W ratio to determine its crack growth rate based on constant amplitude load. The virtual crack closure technique tool in MSC Marc/Mentat software with adaptive and global remeshing is applied to assess high cycle fatigue crack propagation using the SENT model. The crack growth pattern for the 3-dimensional simulation characteristics is similar with that of the CT Specimen experimental procedure. Furthermore, the results of the crack propagation and the cycle count demonstrated good agreement with bearable discrepancy with maximum percentage difference of about 14.1 % for the HAZ and 6.4% for the weld and parent metal compared to the experimental results from literature.

Keywords: Crack growth, structural steel, single edge notched tension, finite element method, MSC Marc/Mentat

1. Introduction

Deterministic and probabilistic fracture mechanics have recently become increasingly acceptable for realistic assessment of fatigue resistance response and reliability of fatigue crack growth rate (FCGR) in steel structures. The implication of crack in engineering component undermines the ultimate allowable stress of the component, as the strain at a sharp crack tip or crack front tends to infinity. The linear elastic fracture mechanics method estimates fatigue damage parameters such as stress intensity factor (SIF) or J-integral and this parameter is related to the FCGR [1]. High strength low alloy (HSLA) steel with light-weight and reserve strength such as API 5L X780 is mostly used in the

*Corresponding author: lanrebusari@gmail.com

2021 UTHM Publisher. All rights reserved.

penerbit.uthm.edu.my/ojs/index.php/ijie

manufacturing of oil and gas structures, in spite of its good weldability, their overall strength is lessened when welded. The weld zone portends severe hardness, crack growth due to metallurgical transformation which is detrimental to the structural integrity [2][3]. Therefore, the fatigue crack is of greater interest due to the short elastic mode. The need for a suitable small-scale yielding specimen is desired at the region where the linear elastic fracture mechanics (LEFM) principle is valid with Paris law. Fatigue crack growth rate prediction is essential to enhance service life for engineering structures, then engineering critical assessment may support decisions that can help to avoid costly repair while advanced reliability analysis technologies is engaged [4][5]. Since probability methods are used to determine the system reliability as the basis for decision-making, the use of existing quality criteria is generally over-conservative with regard to permissible defects. The LEFM was initially developed as illustrated in BS7910 for this purpose using the knowledge of reliability [6]. LEFM is capable of describing crack growth in high strength steel (HSS) structures in a physically correct way [7][8]. The crack will progress provided the SIF (K_I) exceeds the material fracture resistance K_{IC} [9][10]. The SIF varies with the specimen crack length, geometry and load applied depending on loading condition and sequence. In FEM simulations, the reliability LEFM analysis of FCGR in structural components depends on the fatigue crack parameters. However, such crack growth rate parameter is usually obtained experimentally.

Most literature agreed that the prediction of FCGR by using Paris law requires the determination of appropriate parameters of the growth rate curve associated with material properties, types of welded joints for geometry function and calculation of the SIF range (ΔK). The significance of specimen geometry and the stress intensity range is described in Burgel et al. [11]. The long, slender double-cantilever beams (DCB) exhibit higher load drops and prolonged constant stress intensity (K) response time than compact tension (CT) geometry. Furthermore, the single edge notched (SEN) specimen which are narrower demonstrate lesser load drop as the crack approaches the specimen boundary, the dynamic stress intensity may not exceed the static value. Thus, the specimen geometry can be manoeuvre with considerable freedom to achieve the desired crack growth behaviour. Finite element and parameter analysis is used to accomplish the most appropriate specimen design for a given application. The probability model conceptualizes the uncertainty of crack size, loads, and material properties, when carefully modelled, this influences the integrity of cracked structures. Experimental studies have shown that the use of notched specimen to generate a fatigue crack with cyclic loading via the pin placed between the hole in compact tension specimen [12,13]. However, the actual stress under the pin load is not concentrated and much lesser than the stress near the crack tip with stress concentration, hence, its effect on the crack tip can be ignored in finite element method [14]. The single edge notch tension (SENT) specimen has been investigated by [15–17] it could examine the transferability between standardized small-scale geometry specimen and full-scale conditions [18] and moderate representation of fracture mechanics to numerically predict damage and crack propagation between maintenance intervals particularly when the SIF is not available, FE calculations should be considered [19,20]. The basic concern with finite element method (FEM) implementation is for efficient estimation of the SIF values during each FCG cycles of maximum and minimum applied load [21]. Shivakumar K.N *et al.* demonstrated the use of VCCT for the measurement of SIFs for cracked three-dimensional bodies [22].

There is a wide range of literature dealing with the prediction of welded steel as it affects the fatigue crack propagation properties and fracture parameters in small-scale specimens with conventional compact tension and single edge notched bending. Researches have shown that metallurgical factor, position of notch and crack initiation all affect the values of the stress intensity range and Paris Law parameters in the Paris' equation (i.e. fatigue crack parameter C and m) [23–29], therefore the intended service condition play a major role in the fatigue resistant behaviour of high strength steels. In most cases, the load characteristic of conventional specimen does not reflect the reality in many structural or component loading. Nevertheless, the use of fatigue crack parameter from conventional specimen for SENT model in numerical analysis of fatigue crack growth rate (FCGR) related work is rare. This effort could avail the industrial community the lead way to harnessing numerical computation of complex structure by its implementation.

Considering the feasibility of FEM modelling in SENT specimen, the mesh has to be compatible across the crack more precisely and singular stress field at crack tip requires special elements or meshing techniques to be modelled with good accuracy and the force directly at the crack tip. FEM simulation tools have also established the varying SIF along the crack-front subject to the thickness and the ratio of crack length to specimen thickness (a/W) [30][31]. Andrzej Leski (2007) performed 3D VCCT with FE analysis the database stored in the pre and post-processing FE software that provides solid modelling, meshing, analysis setup, while the 3D VCCT is cooperated into some other FE solvers [32]. A commercial software MSC Marc/Mentat [33] VCCT is engage to estimate components of the strain energy release rate (G) at the crack front in the finite element estimation of SIFs by an updated crack closure integral. More so, the process of remeshing as the crack propagates modifies the crack tip profile substantially, allowing strain energy release rates to be calculated using simple equations of a single FE analysis with VCCT in either crack tip or front for 3D. The stress intensity agrees strongly with the crack energy release rate in linear elastic condition [34]. The energy release rate is estimated with forces and displacements around the crack tip in VCCT [33]. Finite element method for LEFM estimation of FCGR in structural components can only be valid as the fatigue crack growth parameter that is input into the simulations. Such crack growth rate data are usually obtained on standardized specimens from experimental procedures.

Crack propagation may be studied using energy release rate (G), however the current methods are not usually precise, effective, or complex. The finite element approach demands fine element mesh that can conform with geometry of the crack front. Many complex geometry situations are challenging while the remeshing is computationally costly in propagation, and inaccuracies in G are exacerbated. The novel spring model that inserts stiffness springs at the crack front and back to compute G using the VCCT is one approach to this drawback. A new interface element is used as shape functions to move the springs to the crack front location that produce accurate forces and displacements. The precise calculation of G along the crack front is essential for appropriate propagation computation. The Surface crack initiator in MSC Marc is implemented with local and global adaptive remeshing process of crack growth numerical analysis which was validated with experiment results.

In FEM analysis of FCG, the modelling of the moving crack requires adaptive local remeshing element to deal with the singularity field is one of the basic issues[35]. The remeshing at cycle interval and faceted surface in MSC Marc/Mentat for local mesh adaption could resolve the element type constraints highlighted by Areias P *et al* [36,37]. In this study, the suitability and reliability of a VCCT based finite element model is implemented for crack growth in mode (I). The method of adaptive local and global remeshing for the crack propagation in SENT model under cyclic loading at constant amplitude for API 5L X70 Steel. The research effort describes the crack length and growth pattern related to the number of load cycles for the stress ratio R=0.1 with respect to the energy release rate at the crack front. The fatigue crack parameter and material properties used was obtained from literature [38] determined experimentally from compact tension specimen. The accuracy and consistency are evaluated and compared with theoretical analysis in this work and experimental work from literature.

2. Numerical Modelling for Fatigue Crack Propagation

The energy needed to advance a crack is equivalent to the amount required to close the crack. Another assumption of VCCT is that the crack tip displacements and energy state is not altered significantly between two successive crack extensions [39]. Rybicki and Kanninen created the approach for 4-noded 2D elements and Ramamurthy T.S. et al. [40] came up with the method of quadratic 8-noded non-singular and quarter node 2D elements. Furthermore, Raju I. S. [41] proposed singularity 2D and 3D elements method with cubic 12-noded with the VCCT formulas depending only on forces and displacements around the crack tip. The linear elastic fracture mechanic concept of crack propagation for planar crack is possible once the energy released for unit width and length of fracture surface (Δa) is termed strain energy release rate (G) proportional to fracture toughness characteristics of the material [42]. The computation of G is usually implemented together with FEM by VCCT by the assumption of small crack extension. The strain energy released is equal to the amount of the work (W) required to close the crack which is evaluated by the stress field and the displacement of the crack front extension from $a+\Delta a$. Furthermore, the stress and displacement can be computed within the same configuration in a single analysis, then G can be expressed as Equation 1:

$$G = \lim_{\Delta a \rightarrow 0} \frac{W}{\Delta a} \tag{1}$$

The displacement and stress at the crack tip is correlated to G for isotropic material, the applicability of the crack closure integral theory for interface failure of stress components is further achieved [43,44]. Irwin presented the crack closure integral theory, which is an energy conservation argument on crack extension generally expressed as:

$$G_I = \frac{1}{2\Delta a} \int_0^{\Delta a} \sigma_y(\Delta a - r, 0) \Delta v(r, \pi) dr \tag{2}$$

The distance from the crack tip to point of surface crack is (r), this distance of crack extension is (Δa) and the displacement in the y-direction is represented with (Δv) during the crack extension when the normal stress (σ_y) is acting along the closed crack surface (line). For 3D VCCT, Equation 2 was modified by Shivakumar *et al* [22] as Equation (3).

$$G_I = \frac{1}{2w_i\Delta a} \int_{s_{i+1}}^{s_{j+1}} \int_0^{\Delta a} \sigma_y(r, \pi) \Delta v(\Delta a - r, 0) dr ds \tag{3}$$

Where (w_i) is element length while (s) is distances along the crack front. The Fig. 1 and the for an 8-node element in the Equation (4) is the results of the node forces (F) ahead of the crack front and the node displacements behind the crack front for the i_{th} segment with contributions for elements on each side of the crack front.

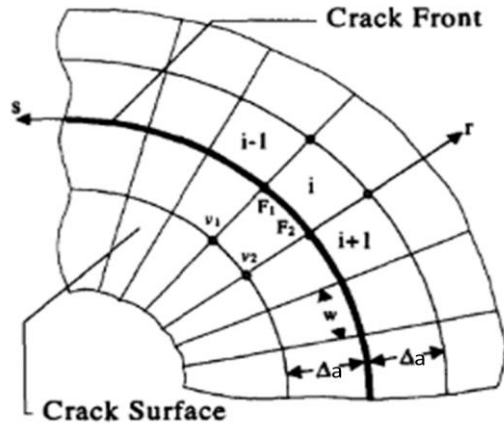


Fig. 1 - Schematic crack plane parameters for computation of energy release rate [45]

$$G_I = \frac{1}{2wi\Delta a} \sum_{j=1}^2 C_j F_j \Delta v_j \quad (4)$$

For 3-D solids condition depicted in Fig. 2, the evaluation is done separately for each node along the crack front for an Area given by the shaded part in MSC Marc/ Mentat. For the case of higher-order elements, the contributions from the mid-side nodes included as obtained Equation (5) using the notation in Fig. 3.

$$G = \frac{F_1 U_1 + F_2 U_2 + \frac{1}{2}(F_3 U_3 + F_4 U_4)}{2a} \quad (5)$$

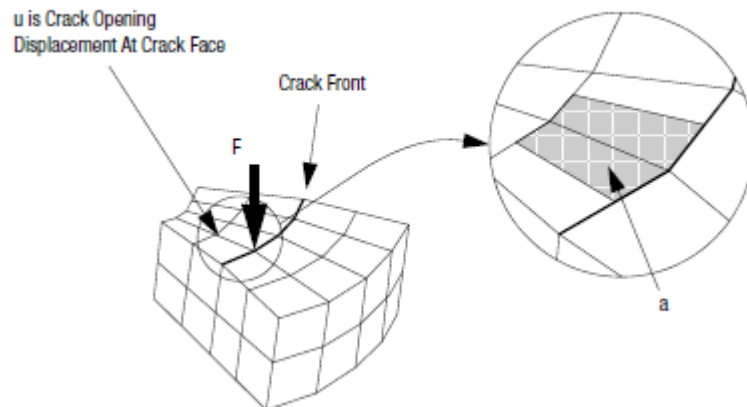


Fig. 2 - 3-dimension mesh for VCCT

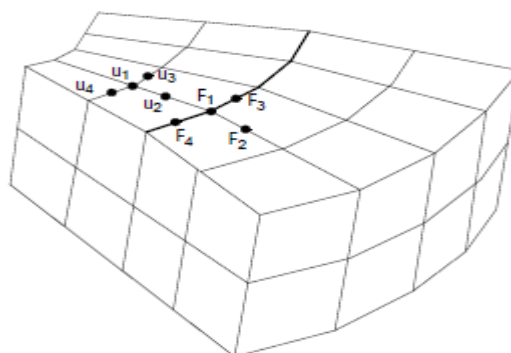


Fig. 3 - 3D mesh for VCCT for higher order mesh elements

Recent research on welded high strength steel components prediction mostly engage LEFM based on Paris' law fitted to fatigue tests [46][47]. The implementation of LEFM evaluates the fatigue strength of defined crack with the assumption of elastic material behaviour during the fatigue process. In LEFM, the most vital driving force for the fatigue crack propagation of HSS is the (G) or SIF (K). For a consistent stress field, Equation (4) is valid and approximate for a stress field that is not uniform. Provided the forces come from nodes on the crack front, and the distance from nodes behind the crack front. In the case of 2-dimension virtual crack closure technique where all elements around the crack tip have the same shape and size. To ensure all elements around the crack front have the same shape and size in 3-dimensions VCCT, the basic approach is to engage higher order elements in finite element analysis in order to enhance its accuracy [22][32]. In Finite element analysis, the required potential to close the crack over a surface area is the local (G). Furthermore, these equations are used to obtain the full (G) in FEA. Then SIF (K_I) in mode I can be determined with the equations presented in Equation (6) in plane strain and plane stress in Equation (7) respectively:

$$G_I = \frac{K_I^2}{E} (1 - \nu^2) \xrightarrow{\text{yields}} K_I = \sqrt{\frac{G_I E}{1 - \nu^2}} \tag{6}$$

$$G_I = \frac{K_I^2}{E} \xrightarrow{\text{yields}} K_I = \sqrt{G_I E} \tag{7}$$

The (ν) represents the poisson ratio and (E) denotes the elastic modulus in the equations. In numerical FEM modelling, where the propagation direction might not be implemented, remeshing techniques are required [48–51]. Marc offers the evaluation of fracture mechanics based on the energy release rate with VCCT for crack. The application of VCCT is useful as it provides G to be calculated using simple equations from a single FE analysis. The VCCT is one of the most common tools to evaluate G components along a crack front in linear elastic condition. The postulation of a crack is a crack tip for 2-dimension and a crack front in 3-dimension. For either crack model, the J-integral or a VCCT calculation is to be performed. The energy release and SIF is a fundamental parameters of fracture mechanics, for the single edge notch tension specimen, the SIF represents stress condition at a crack tip, is proportional to crack growth rate and is used to assess failure criteria due to fracture stress, where in mode I failure analysis is established analytically by Equation (8).

$$K_I = \delta \sqrt{\pi a} \cdot f\left(\frac{a}{W}\right) \tag{8}$$

Various empirical formulas of geometry functions $f(a/W)$ in terms of determining SIF for different types of specimens already presented by many researchers. In this paper, the formula for the correction factor for SENT specimen is applied using this Equation (9)[52][53].

$$f = 1.12 - 0.231\left(\frac{a}{W}\right) + 10.55\left(\frac{a}{W}\right)^2 - 21.72\left(\frac{a}{W}\right)^3 + 30.39\left(\frac{a}{W}\right)^4 \tag{9}$$

The crack grows when the G or the SIF is equal to the critical value of the component, the cycle count of crack growth to reach a critical length is a function of the SIF range (ΔK) or SIF (K_I).

$$\frac{da}{dN} = C(\Delta K)^m \tag{10}$$

$$dN = \frac{da}{C(\Delta K)^m} \tag{11}$$

$$\int_0^{Nf} dN = \int_{a_i}^{a_f} \frac{da}{C(\Delta K)^m} \tag{12}$$

The SIF range of the material/ crack tip of constant amplitude loading from equation (8) is substituted.

$$\int_0^{N_f} dN = \frac{1}{C} \int_{a_i}^{a_f} \frac{da}{(f\Delta\delta (\pi a)^{\frac{1}{2}})^m} \tag{13}$$

The number of load cycles for each increment is given as:

$$N_f = \frac{a_{i+1}^{(1-0.5a)} - a_i^{(1-0.5a)}}{C(f(\Delta\delta)\pi^{\frac{1}{2}})^m (1 - 0.5m)} \tag{14}$$

The material constant is (C and m) and K is SIF which is expressed in the previous equation. However, the fatigue crack growth of difference welding procedure mainly caused the variation of material parameters in the HAZ [54].

2.1 3-Dimensional VCCT Numerical Analysis

The resources of fracture mechanics in MSC marc entail the assessment of the energy release rate with automatic crack propagation using the VCCT option. Crack displacement and stress methods require orthogonal mesh around the crack front to obtain accurate SIF solutions, due to the changing geometrical requirements, a great deal of care must be taken in creating the mesh pattern on and near the crack plane [45]. MSC Marc/Mentat provide finite element analysis VCCT method with remeshing of crack propagation. For isotropic linear elastic material, Marc calculates the SIF from the energy release rate. This is done separately for each crack mode. With the J-integral the calculation of the SIFs is more complex, and it is only done if there are no point forces in the crack region. Contact forces from self-contact at the crack faces are also included in these point forces, which means that the calculation of K factors is not available if self-contact is included. It is possible in Marc to omit the check for self-contact, with the risk of material overlap in case the crack closes. In fatigue analysis, a repetitive load and the main goal is typically to find the amount of load repetitions it takes to grow a crack to a certain length. The number of load cycles is often huge, much more than one would explicitly model in the analysis, this is called high cycle fatigue. The speed or rate of crack growth is given by a fatigue law, and Marc uses the typical Paris' law. In direct growth crack propagation, nothing happens with the crack until a crack growth criterion is fulfilled [33].

The 3D fatigue crack growth evaluation by FEM has been made on SENT specimen using MSC Marc/Mentat commercial finite element software. The tested CT specimens were remodeled into SENT specimens using the material properties of API 5L X70 grade steel obtained from the literature[38] as listed in Table 1 and 2. The specimen geometry considered in this analysis with match crack depth of the SENT model is shown in Fig. 4. The geometry function (a/W) has been taken as 0.2, the crack length is (a). The specimen width (W) and thickness are constant for the entire analysis.

Table 1 - A Material properties o of API 5L X70 grade steel obtained from the literature[38]

Young modulus (GPa)	Yield Strength (MPa)	Thickness (mm)	Poisson ratio
221	500.3	7	0.3

Table 2 - Paris law constant in the different zone obtained from the literature [38]

	C	m
Base metal	1.1e ⁻¹¹	4.87
Heat affected zone	8.1e ⁻¹¹	3.82
Weld metal	5.2e ⁻¹¹	4.55

The finite element of SENT specimen was considered for crack front deformation analysis, using MSC Marc/Mentat has been modelled using 72,000 elements and 24,558 nodes with quad-meshing. Displacement controlled tensile load has been applied on the upper edge of the specimen. Because of strain variations, the model employs the patran tetra remeshing approach. One of the criteria to significantly enhance the accuracy of VCCT in FE analysis is to use higher-order elements One of the conditions to improve the accuracy of the FE analysis in VCCT is to utilize higher order elements [32,55,56]. The complicated singularity of the stress field at the fracture front necessitates the production and regeneration of a dense mesh as the crack develops [58]. The quad (8) model was changed to tetra (4) element in Fig. 5 to avert the complexities of the phenomenon of element type alteration in simulation. The global remeshing criteria's is assign to the contact bodies. In Fig. 5(b), the faceted surface used to describe of the stress fields, that is significant to determine the crack path and singular elements is simply meshed round the crack front. The assign SENT model is remeshed to the standard remeshing criteria since crack propagation promptly triggers remeshing

automatically. Also, the mesh density control for the target element edge length was set at 2 mm. The material SIF describes the stress on crack tips and the crack growth caused by external loads or inherent stress in fracture mechanics. This includes the size of the workpiece, initial crack length and yield strength.

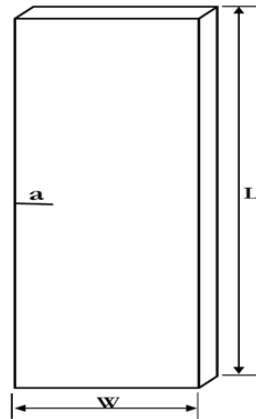


Fig. 4 - Geometry model for SENT in MSC Marc/Mentat

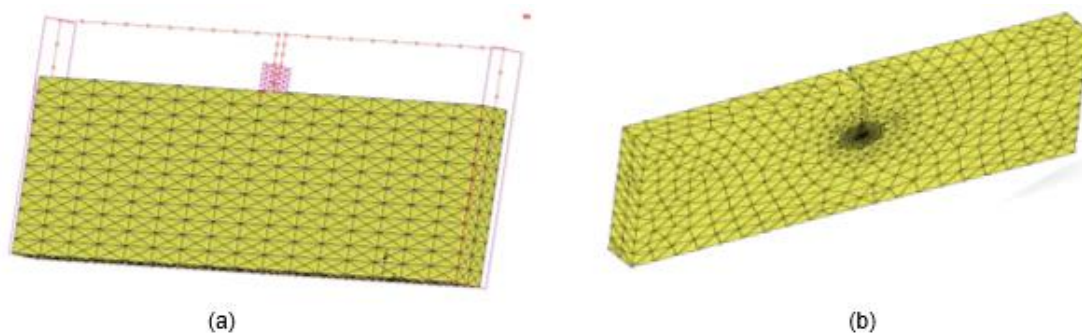


Fig. 5 - FE modelling geometry model for SENT in MSC Marc/Mentat. (a) clipped model of crack faceted surface orientation with Quad (8) meshing; (b) crack front propagation with patran tetra remeshing

The model was characterized as a contact body with deformable body properties that allow deformations to move easily within the contact body alongside the faceted nodes in the centre of the model perpendicular to the surface is used to define the crack path. The SIF is computed based on the Paris law with the periodic high cyclic loading. Furthermore, the fatigue time period of the repeated load sequence and the crack growth increment is assigned and input for the fatigue crack parameters m and C were obtained from literature from CT specimen experimental fatigue tests Table 2. The initial state is structural, with boundary and loading parameters selected to replicate experiment situations with cyclic load is applied in the x-axis direction (58 MPa) in the right end of the model, while the fixed displacement is applied in the left end of the model to imitate clamping condition as illustrated in Fig. 6(a). The constant amplitude with the mode I tensile load is implemented normal to the crack face on the free edge of the model and the sine based cyclic load table with the stress ratio $R=0.1$ in Fig. 6(b) is assigned as expressed in Equation (15).

$$f(t)=0.45*\sin(2*\pi*v1-(\pi/2)) + 0.55 \quad (15)$$

Crack growth increment 0.2 mm is chosen to shorten the computational time. The evaluation of rate of energy release in VCCT through the forces and the displacements along the crack front is implemented in the load case created for all the conditions loads by means of a persistent time step of 0.5 seconds per increment. Sufficient total load case and time Steps were chosen to allow for suitable visualization of the simulations, this input values were varied to assess the effect on the computation outcome.

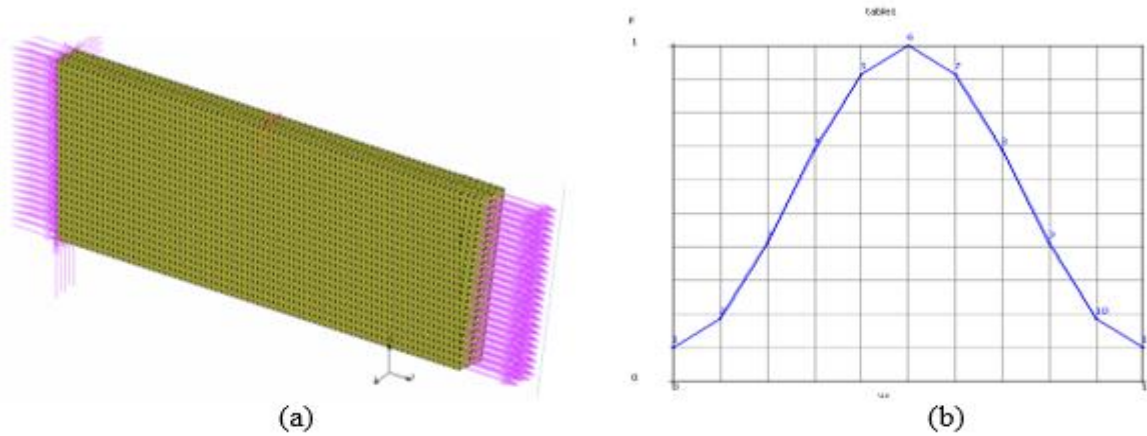


Fig. 6 - (a) Load boundary condition of the specimen with one end fix and other side cyclically loaded; (b) cyclic Load table at stress ratio R=0.1

2.2 Mesh Sensitivity

Linear Elastic Fracture Mechanics in FEM represented the most advanced theory for simulating crack growth. However, the element size around the discontinuity must be small enough to capture a stress variation and the consequence is the computational time. Hence, the investigation of the crack propagation effect is performed using the same parameters but lesser crack length (load case) for simplicity. The simulation is carried out in 3D solid FEM model, by creating a batch file (.bat) coding in MSC Marc/Mentat. The script enables multiple meshes to run with less computer memory consumption. For the analysis procedure, a direct solver has been employed to run the solid mechanic computation with a multi-frontal parallel sparse algorithm. Also, the software-running environment is the 64-bit WIN10 system with a 12-GB RAM, CPU 3.10 GHz, and Intel-i5 processors. Firstly, mesh size dependency on the crack growth rate and corresponding load cycles, created multiple (.mud) files with different mesh size/number of elements in Table 3. Secondly, remeshing mesh size behaviour was computed for the equivalent number of load cycle and computation time of chosen mesh size, as presented in Table 4.

Table 3 - Mesh size sensitivity analysis

Mesh Size	No. of load cycles (mm/cycle)	Computation Time (sec)
0.25	489831	6294.56
0.5	597516	2035.19
1	489558	2051.07
2	490572	2009
4	490455	2021

Table 4 - Remeshing size sensitivity analysis with mesh size of 2mm

Mesh Size	No. of load cycles (mm/cycle)	Computation Time (sec)
0.5	486616	3194
1	488719	1512
2	490545	2071
3	84534	2110
4	242934	2032

3. Results and Discussion

The analysis describes the findings of FCG derived from the computational method. It should be noted that the SIF values in an automated crack simulation like MSC Marc/Mentat is computed centered around fracture energy release rate according to cyclic load table in Fig. 6 and Equation (15). The software evaluated the energy release rate with

Equation 6 and 7 according to the isotropic material. The corresponding mean value elastic modulus and Poisson ratio in the literature [38] for welded, base metal and HAZ is used. Furthermore, a minimum of crack length was created in the load case based on ASTM standard [58], the constant time step aimed to represent the crack growth and remeshing of nodes from the initial crack at every 0.2 mm for each step and nodes are released subsequently. Hence, the crack progresses by 0.2 mm till the last targeted length is achieved. Counter plots show the interaction effect of the clamping force on the model on the left side presented in Fig. 9 which causes almost uniform stress distribution in the whole mode region that normal leads to uniform crack propagation without the effect of bending deformation. However, as the crack progresses the cyclic load effect is prevalent mostly on the right-hand side where the load is applied in Fig. 8 and Fig. 9.

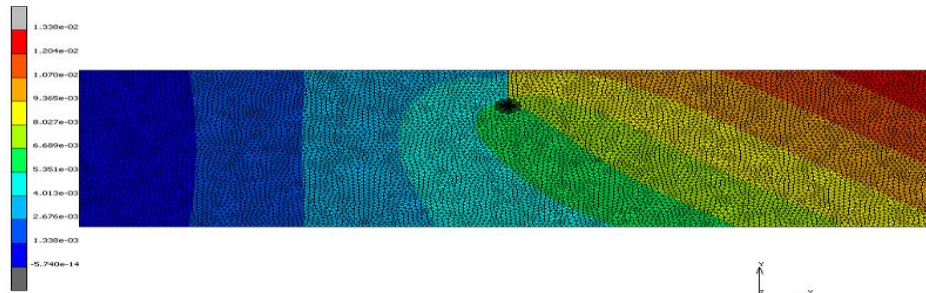


Fig. 7 - Model plot for crack growth at initial increment

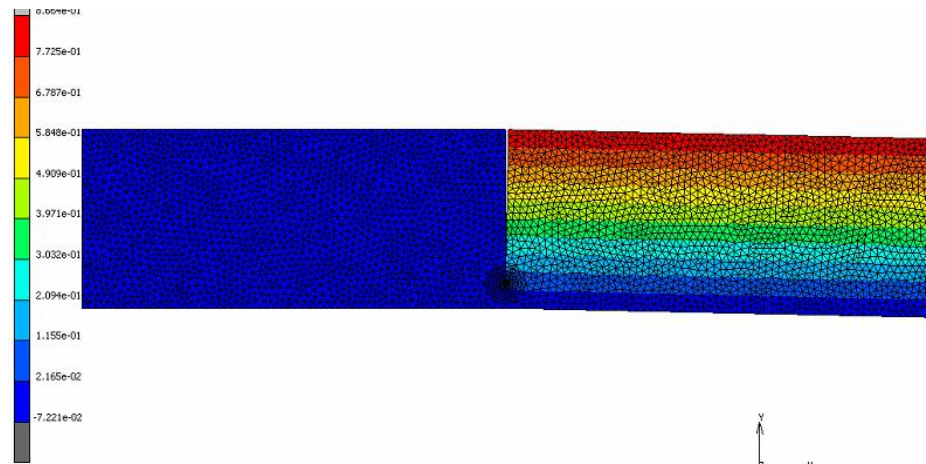


Fig. 8 - Model plot for crack growth as increment progresses

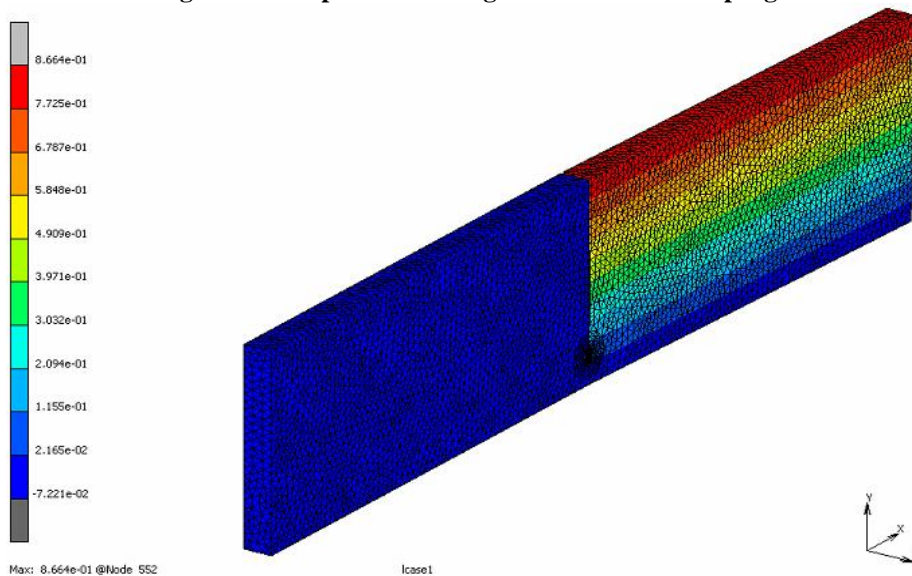


Fig. 9 - 3D Model plot crack growth increment

The relation of fatigue crack growth along the length of element starting from 10mm which includes the size of initial crack length versus the cycles count between the SENT model finite-element approach as shown in Fig. 10. The number of load cycles of FCG studied with experimental CT specimen and the FE analysis of SENT specimen with MSC Marc/Mentat, using VCCT is presented in Table 5. The ratio of fatigue crack geometrical function $a/W=0.2$, and the fatigue crack parameter of CT specimen employed demonstrates a feasible SENT specimen application. However, the reason for an evident variation in the value number of loads cycles of the HAZ is not clear. However, it may be influence by inherent stress or the possibility of grain size refinement of the material not adequately account for in the simulation. Several literatures describe the metallurgical variables linked to the welding process and the heat input have a more uncertain effect on the fatigue characteristics of HAZ that could account for crack pattern observed in this work.

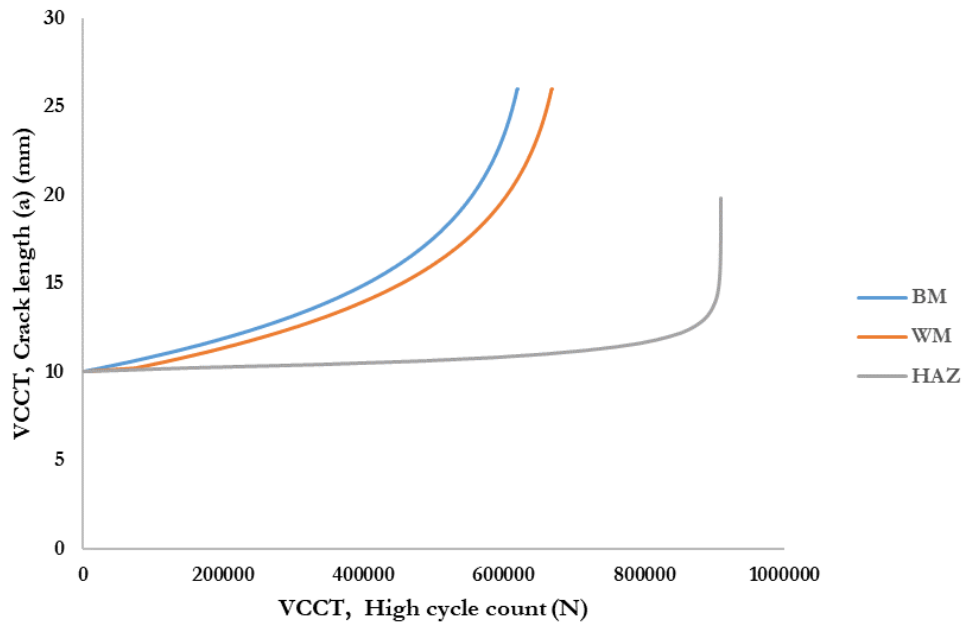


Fig. 10 - VCCT crack length and number of cycles count with SENT model

The possibility of adverse microstructure, grain refinement and martensite formation in the HAZ of welding high strength steel, which might account for different flow stresses at different zones of the welded steel plates where the fatigue crack parameter was obtained experimentally with compact tension specimen for this numerical analysis. The constant amplitude loading with high cycle fatigue was performed at the same conditions of ΔK and K_{max} for all the weld zone based on the cyclic loading table presented in the figure above. Contrary to other cracks growth in Fig. 10, the sluggish fatigue crack propagation experienced in the VCCT simulation for the HAZ with the same condition of stress intensity, the crack propagation in the HAZ, BM and WM regions for the steel may be as a consequence of a material hardness, particularly the (HAZ). The value of C and m is treated as the material properties of each region [59], therefore the residual stress effect is expected to be captured.

Table 5 - Number of times and cycles of FCG simulated with SENT model vs. CT experiment result

Specimen	Crack length (mm)	No. of cycles (BM) (mm/cycle)	No. of cycles (HAZ) (mm/cycle)	No. of cycles (WM) (mm/cycle)
Experiment CT[38]	25	6.6×10^5	7.7×10^5	7.15×10^5
Numerical computation with SENT	25	6.17×10^5	9.0×10^5	6.67×10^5
Percentage Difference		6.1%	14.4%	6.4%

4. Conclusion

An advanced global remeshing criteria is used in the VCCT to propagate cracks in FE analysis. The SENT model of the crack growth of high strength steel samples performs high cycle fatigue in MSC Marc/Mentat. The convergence analysis illustrates the potential and reduces the inaccuracy and computational time of the model. Summarily, the single edge notched tension crack model has been implemented and compared with the values of compact tension specimen in the experiment. This study also demonstrates that numerical solution is a proficient tool for a conservative estimation of the fatigue life provided the fatigue crack parameter is available for the LEFM approach with constant amplitude fatigue loading. Some conclusions can be drawn from the current comparisons of published experimental data and computation solutions as follows:

- The SENT prediction models implemented is verified with the experimental results with similar loading condition procedures alongside a considerate continued meshing convergence.
- A phenomenon of adaptive remeshing in VCCT follows the trends of LEFM in crack incremental summation except in the HAZ.
- The 3D-simulation results of the computed crack length and equivalent cycle counts with same applied load of 62.5MPa and stress ratio of $R=0.1$ show acceptable agreement compared to experimental investigation from literature with a percentage difference of 6.1% for base metal, 6.4% for weld metal and highly conservative 14.4% for HAZ structural steels

Furthermore, the VCCT fatigue crack growth observations indicate that the integrity of a welded high strength steel structure can depend on the welding component toughness region particularly in HAZ. Future models could integrate the interfaces between linear and non-linear fracture mechanics or strain hardening in a more complex model. The standardization process of SENT specimen for fatigue crack growth could further enhance more accurate fatigue life prediction.

Acknowledgement

Authors express gratitude for the computational facilities granted by smart manufacturing research institute (SMRI), Universiti of Teknologi MARA, (UiTM), Malaysia.

References

- [1] Chambel, P., Martins, R.F., and Reis, L. (2016) Research on fatigue crack propagation in CT specimens subjected to loading modes I, II or III. *Procedia Structural Integrity*. 1 134–141
- [2] Ribeiro, H.V., Reis Pereira Baptista, C.A., Fernandes Lima, M.S., Santos Torres, M.A., and Marcomini, J.B. (2021) Effect of laser welding heat input on fatigue crack growth and CTOD fracture toughness of HSLA steel joints. *Journal of Materials Research and Technology*. 11 801–810
- [3] Sorrija, B.A. and Nascimento, M.P. (2015) Fatigue crack growth rate analysis in an API 5L X70 steel pipe. in: *Rio Pipeline Conference and Exposition, Technical Papers*,
- [4] Al-Mukhtar, A.M., Biermann, H., Hübner, P., and Henkel, S. (2010) Determination of some parameters for fatigue life in welded joints using fracture mechanics method. *Journal of Materials Engineering and Performance*. 19 (9), 1225–1234
- [5] Zhang, X., Gao, H., and Huang, H.Z. (2018) Total fatigue life prediction for welded joints based on initial and equivalent crack size determination.
- [6] Nasir, N.N.M., Abdullah, S., Singh, S.S.K., Haris, S.M., and Zainal, S.S.M. (2018) The Need to Evaluate Reliability Based Fatigue Data. *International Journal of Engineering & Technology*. 7 1491–1495
- [7] Irwin, G.R. (1957) Analysis of stress and strain near the end of a crack traversing a plate. *Journal of Applied Mechanics ASME*. 24 361–364
- [8] Alam, M., Barsoum, Z., and Jonsén, P. (2009) Fatigue behaviour study of laser hybrid welded eccentric fillet joints–Part II: State-of-the-art of fracture mechanics and fatigue analysis of welded joints. *Proceedings of ...* 1–33
- [9] Tada, H., Paris, P.C., and Irwin, G.R. (1985) *The Stress Analysis of Cracks Handbook*. third ASME Press, New York
- [10] Paris, P. and Erdogan, F. (1963) A critical analysis of crack propagation laws. *Journal of Basic Engineering. TransAmSocMech Eng*. 85 (4), 528–534
- [11] Bürgel, A., Kobayashi, T., and Shockey, D.A. (2003) Laboratory test for measuring resistance to rapid crack propagation. *European Structural Integrity Society*. 32 (C), 175–185
- [12] Newman, J.C., Yamada, Y., and James, M.A. (2011) Back-face strain compliance relation for compact specimens for wide range in crack lengths. *Engineering Fracture Mechanics*. 78 (15), 2707–2711
- [13] Newman Jr, J.C. (2000) Advances in fatigue and fracture mechanics analyses for metallic aircraft structures. *NASA Scientific and Technical Information (STI) Program. NASA/TM-20 45*
- [14] Duan, C., Chen, X., and Li, R. (2020) The numerical simulation of fatigue crack propagation in Inconel 718

- alloy at different temperatures. *Aerospace Systems*. 3 (2), 87–95
- [15] Simunek, D., Leitner, M., and Grün, F. (2018) In-situ crack propagation measurement of high-strength steels including overload effects. *Procedia Engineering*. 213 (2018), 335–345
- [16] Verstraete, M.A., De Waele, W., Van Minnebruggen, K., and Hertelé, S. (2015) Single-specimen evaluation of tearing resistance in SENT testing. *Engineering Fracture Mechanics*. 148 324–336
- [17] Weeks, T.S. and Lucon, E. (2014) Direct comparison of single-specimen clamped SE(T) test methods on X100 line pipe steel. *Proceedings of the Biennial International Pipeline Conference, IPC*. 4 (October 2014),
- [18] Weeks, T.S. and Read, D.T. (2015) Comparison of J-integral from single specimen SE(T) tests on API-5L X100 line pipe steel. *Proceedings of the International Offshore and Polar Engineering Conference*. 2015-Janua (June 2015), 592–601
- [19] Busari, Y.O., Ariri, A., Manurung, Y.H.P., Sebayang, D., Leitner, M., Zaini, W.S.B.W., et al. (2020) Prediction of Crack Propagation Rate and Stress Intensity Factor of Fatigue and Welded Specimen with a Two-Dimensional Finite Element Method. {IOP} Conference Series: Materials Science and Engineering. 834 12008.
- [20] Schijve, J. (2009) Fatigue Crack Growth. Analysis and Predictions. in: J. Schijve (Ed.), *Fatigue of Structures and Materials*, Springer Netherlands, Dordrechtpp. 209–256
- [21] Rege, K. and Lemu, H.G. (2017) A review of fatigue crack propagation modelling techniques using FEM and XFEM. *IOP Conference Series: Materials Science and Engineering*. 276 (1),
- [22] Shivakumar, K.N., Tan, P.W., and Newman, J.C. (1988) A Virtual Crack-Closure Technique for Calculating Stress Intensity Factors for Cracked Three Dimensional Bodies. *International Journal of Fracture*. 36 43–50
- [23] Jacob, A., Mehmanparast, A., D'Urzo, R., and Kelleher, J. (2019) Experimental and numerical investigation of residual stress effects on fatigue crack growth behaviour of S355 steel weldments. *International Journal of Fatigue*. 128 105196
- [24] Kucharski, P., Lesiuk, G., and Szata, M. (2016) Description of fatigue crack growth in steel structural components using energy approach - Influence of the microstructure on the FCGR. *AIP Conference Proceedings*. 1780 0–8
- [25] Milović, L., Vuherer, T., Radaković, Z., Petrovski, B., Janković, M., Zrilić, M., et al. (2011) Determination of fatigue crack growth parameters in welded joint of HSLA steel. *Structural Integrity and Life*. 11 (3), 183–187.
- [26] Carpinteri, A., Ronchei, C., Scorza, D., and Vantadori, S. (2015) Fracture mechanics based approach to fatigue analysis of welded joints. *Engineering Failure Analysis*. 49 67–78
- [27] Kim, B.J. and Lim, B.S. (2004) Microstructure and fatigue crack growth behavior of heat affected zone in P92 steel weldment. *Key Engineering Materials*. 261–263 (II), 1185–1190
- [28] Kim, S., Jeong, D., and Sung, H. (2018) Reviews on factors affecting fatigue behavior of high-Mn steels. *Metals and Materials International*. 24 (1), 1–14
- [29] Kim, S., Kang, D., Kim, T.W., Lee, J., and Lee, C. (2011) Fatigue crack growth behavior of the simulated HAZ of 800MPa grade high-performance steel. *Materials Science and Engineering A*. 528 (6), 2331–2338.
- [30] Xin, H. and Veljkovic, M. (2020) Residual stress effects on fatigue crack growth rate of mild steel S355 exposed to air and seawater environments. *Materials and Design*. 193 108732.
- [31] Kodancha, K.G. and Kudari, S.K. (2009) Variation of stress intensity factor and elastic T-stress along the crack-front in finite thickness plates. *Frattura Ed Integrità Strutturale*Frattura Ed Integrità Strutturale. 3 (8), 45–51.
- [32] Leski, A. (2007) Implementation of the virtual crack closure technique in engineering FE calculations. *Finite Elements in Analysis and Design*. 43 (3), 261–268.
- [33] MSC Software (2016) Volume A: Theory and user information, 2016.
- [34] Anderson, T.L. (2005) *Fracture mechanics : 3rd Editio* Taylor & Francis., Boca Raton, FL.
- [35] Adak, D., Pramod, A.L.N., Ooi, E.T., and Natarajan, S. (2020) A combined virtual element method and the scaled boundary finite element method for linear elastic fracture mechanics. *Engineering Analysis with Boundary Elements*. 113 9–16
- [36] Areias, P., Reinoso, J., Camanho, P.P., César de Sá, J., and Rabczuk, T. (2018) Effective 2D and 3D crack propagation with local mesh refinement and the screened Poisson equation. *Engineering Fracture Mechanics*. 189 339–360
- [37] Areias, P. and Rabczuk, T. (2017) Steiner-point free edge cutting of tetrahedral meshes with applications in fracture. *Finite Elements in Analysis and Design*. 132 (May), 27–41
- [38] Deliou, A. and Bouchouicha, B. (2018) Fatigue crack propagation in welded joints X70. *Frattura Ed Integrità Strutturale*. 12 (46), 306–318
- [39] Krueger, R. (2004) Virtual crack closure technique: History, approach, and applications. *Applied Mechanics Reviews*. 57 (1–6), 109–143
- [40] Ramamurthy, T.S., Krlshnamurthy, T., Narayana, K.B., Vijayakumar, K., and B. Dattaguru (1986) Modified crack closure integral method for quarter points elements. *Mechanics Research Communication*. 13 (4), 179–186
- [41] Raju, I.S. (1987) Calculation of strain-energy release rates with higher order and singular finite elements.

- Engineering Fracture Mechanics. 28 (3), 251–274
- [42] Janssen, M., Zuidema, J., and Wanhill, R.J.H. (2004) Fracture Mechanics. 2nd ed. Taylor & Francis, .
- [43] Zeng, W., Liu, G.R., Jiang, C., Dong, X.W., Chen, H.D., Bao, Y., et al. (2016) An effective fracture analysis method based on the virtual crack closure-integral technique implemented in CS-FEM. Applied Mathematical Modelling. 40 (5–6), 3783–3800
- [44] Narayana, K.B., George, S., Dattaguru, B., Ramamurthy, T.S., and Vijayakumar, K. (1994) Modified crack closure integral (MCCI) for 3- d problems using 20- noded brick elements. Fatigue & Fracture of Engineering Materials & Structures. 17 (2), 145–157
- [45] Fawaz, S.A. (1998) Application of the virtual crack closure technique to calculate stress intensity factors for through crack with an elliptical crack front. Engineering Fracture Mecahnics. 59 (3), 327–342
- [46] Ottersböck, M.J., Leitner, M., Stoschka, M., and Maurer, W. (2019) Crack Initiation and Propagation Fatigue Life of Ultra High-Strength Steel Butt Joints. Applied Sciences (Switzerland). 9 (21),
- [47] Igwemezie, V., Mehmanparast, A., and Kolios, A. (2018) Materials selection for XL wind turbine support structures: A corrosion-fatigue perspective. Marine Structures. 61 (May 2018), 381–397
- [48] Marco, M., Infante-García, D., Belda, R., and Giner, E. (2020) A comparison between some fracture modelling approaches in 2D LEFM using finite elements. International Journal of Fracture. 223 (1–2), 151–171
- [49] Ferretti, E. (2003) Crack propagation modeling by remeshing using the cell method (CM). CMES - Computer Modeling in Engineering and Sciences. 4 (1), 51–72
- [50] Bouchar, P.O., Bay, F., and Chastel, Y. (2003) Numerical modelling of crack propagation: Automatic remeshing and comparison of different criteria. Computer Methods in Applied Mechanics and Engineering. 192 (35–36), 3887–3908
- [51] Branco, R., Antunes, F.V., and Costa, J.D. (2015) A review on 3D-FE adaptive remeshing techniques for crack growth modelling. Engineering Fracture Mechanics. 141 170–195. London
- [53] Alshoaibi, A. and Ariffin, A.K. (2006) Finite element simulation of stress intensity factors in elastic-plastic crack growth. Journal of Zhejiang University - Science A: Applied Physics & Engineering. 7 1336–1342
- [54] Lassen, T. (1990) The effect of the welding process on the fatigue crack growth. Welding Journal. 69 75S-81S.
- [55] Xie, D. and Biggers, S.B. (2006) Progressive crack growth analysis using interface element based on the virtual crack closure technique. Finite Elements in Analysis and Design. 42 (11), 977–984
- [56] Wang, Y., Waisman, H., and Harari, I. (2017) Direct evaluation of stress intensity factors for curved cracks using Irwin’s integral and XFEM with high-order enrichment functions. International Journal for Numerical Methods in Engineering. 112 (7), 629–654
- [57] Peng, X., Atroschenko, E., Kerfriden, P., and Bordas, S.P.A. (2017) Isogeometric boundary element methods for three dimensional static fracture and fatigue crack growth. Computer Methods in Applied Mechanics and Engineering
- [58] ASTM E 647 –00 (2004) Standard Test Method for Measurement of Fatigue Crack Growth Rates
- [59] Philippe, D., Diego, S., Recho, N., and Tom Lassen (2004) A fracture mechanics approach for the crack growth in weld joints with reference to BS 7910. in: ECF 15